



|                  |  |
|------------------|--|
| Title            | Fatigue crack propagation properties of Ti-6Al-4V in vacuum environments   |
| Author(s)        | Oguma, H.; Nakamura, T.  |
| Citation         | International Journal of Fatigue, 50, 89-93<br><a href="https://doi.org/10.1016/j.ijfatigue.2012.02.012">https://doi.org/10.1016/j.ijfatigue.2012.02.012</a> |
| Issue Date       | 2013-05  |
| Doc URL          | <a href="http://hdl.handle.net/2115/53029">http://hdl.handle.net/2115/53029</a>  |
| Type             | article (author version)   |
| File Information | Fatigue crack propagation properties of Ti-6Al-4V in vacuum environments_HUSCAP-1.pdf  |



[Instructions for use](#)

# Fatigue crack propagation properties of Ti-6Al-4V in vacuum environments

H. Oguma<sup>a, \*</sup>, T. Nakamura<sup>a</sup>

<sup>a</sup> *Division of Mechanical & Space Engineering, Faculty of Engineering,  
Hokkaido University, Sapporo, Hokkaido 060-8628, Japan*

\*Corresponding author.

Tel.: +81 (0)11 706 6421; Fax: +81 (0)11 706 7889; e-mail: Hiroyuki.Oguma@eng.hokudai.ac.jp

## Abstract:

To determine the effects of vacuum environment on fatigue crack propagations in a Ti-6Al-4V alloy, K-decreasing tests were conducted in air and vacuum. The fatigue crack propagation rate became slower and threshold stress intensity factor range became larger with decreasing vacuum pressure. The tendency cannot be fully explained by the crack closure. Based on fracture surface observations, granular region of a few micrometer size asperities was observed on the fracture surface only in high vacuum and ultra high vacuum. The high vacuum environment is one of the necessary conditions for the formation of the granular region, and the fraction of surface coverage of adsorbed gas on fracture surfaces relates to the phenomenon. The formation of the granular region represents the difference of the crack propagation mechanism between vacuum and air environments. A new mechanism for the formation of the granular region was proposed, and that is one of the phenomena which can explain the reduction of crack propagation rate in vacuum.

## Key words:

Fatigue crack growth, Sub-surface fracture, Granular region, Vacuum, Titanium alloy

## 1. Introduction

In recent years, Ti-6Al-4V alloy has been widely used in aerospace industries due to its attractive properties such as excellent specific strength, heat resistance and corrosion resistance. In this material, fatigue properties have been widely investigated [1, 2], and the origin of fatigue fracture is usually at the surface in the high stress and lower fatigue life region, whereas in low stress and longer fatigue lifetimes origins are generally sub-surface in nature [3-5]. One of differences between surface crack and sub-surface crack is environment around them. Sub-surface crack is considered to be exposed to the environment almost without oxidation and gas adsorption, i.e. vacuum-like environment. The properties of the sub-surface fracture have been investigated from the point of view of environment around the fatigue crack [6-9]. Fatigue tests until very high cycle regime were

conducted, and observation of fracture surfaces revealed that a unique fine concave-convex agglomerate (hereinafter called Granular Region) formed on the fracture surface of sub-surface fractures, as shown in Fig.1 [4, 5]. The granular region was not observed on the fracture surface of surface fractures. In vacuum condition, however, the region appears on the fracture surfaces. These results lead to the suggestion that the vacuum environment can affect the formation of the granular region. If the environment around the sub-surface crack is similar to vacuum, there is a possibility that the vacuum-like environment can explain the specific properties of the sub-surface fracture, the appearance of the granular region, as mentioned above. The present work focuses on effects of vacuum environment on the fatigue crack propagation properties in detail, and a mechanism for the formation of the granular region will be proposed.

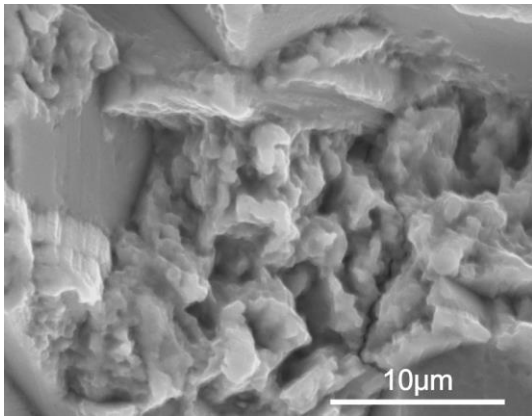


**Fig. 1.** The granular region of the sub-surface fracture (Ti-6Al-4V,  $R = 0.1$ ,  $\sigma_{\max} = 600$  MPa,  $N_f = 5.53 \times 10^7$ ).

## 2. Experimental procedure

### 2.1 Material and specimen

A tested material was ( $\alpha+\beta$ ) Ti-6Al-4V alloy. The chemical composition is given in Table 1. A rectangular bar (25 mm x 50 mm x 1000mm) was made by a gyratory forging machine (GFM) at 1213 K, and underwent the heat treatment of 1203 K, 3.6 ks (1 hr), AC  $\rightarrow$  978 K, 7.2 ks (2 hrs), AC. Mechanical properties after the heat treatment are listed in Table 2. The bi-modal (duplex) microstructure was observed with a scanning electron microscope (SEM), as shown in Fig. 2. The range of primary  $\alpha$  grain sizes is from 5 to 16  $\mu\text{m}$ , and the average size is 10  $\mu\text{m}$ . The range of ( $\alpha+\beta$ ) lamellae length is 4 to 16  $\mu\text{m}$ , and the average length is 10  $\mu\text{m}$ .

**Table 1.**

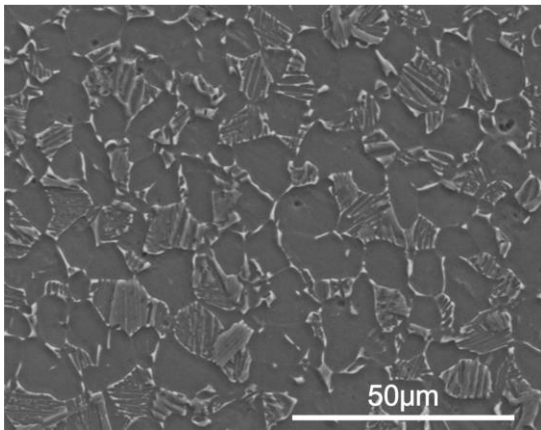
Chemical composition of Ti-6Al-4V (in mass %)

| Al   | V    | O    | N     | C    | Fe   | H      | Ti   |
|------|------|------|-------|------|------|--------|------|
| 6.12 | 4.27 | 0.16 | 0.002 | 0.02 | 0.15 | 0.0029 | Bal. |

**Table 2.**

Mechanical properties of Ti-6Al-4V

| Tensile strength<br>[MPa] | 0.2% proof stress<br>[MPa] | Elongation<br>[%] | Reduction of area<br>[%] | Hardness<br>[Hv] |
|---------------------------|----------------------------|-------------------|--------------------------|------------------|
| 943                       | 860                        | 17                | 40                       | 316              |

**Fig. 2.** Microstructure of Ti-6Al-4V.

The compact tension (CT) specimen was designed according to ASTM-E647-00, and Fig. 3 shows the 25 mm wide and 6 mm thick specimen. A notch was made by an electrical-discharge machining (EDM) perpendicular to the forging direction with a width of 1 mm. The notch root radius was less than 0.25 mm. To remove the hardened layer formed during machining process, both surfaces of the CT specimen were polished with emery paper from #150 to #1500. In addition, observation surface of the specimen was buffed with an alumina abrasive compound until a mirror gloss was obtained to measure the crack length precisely.



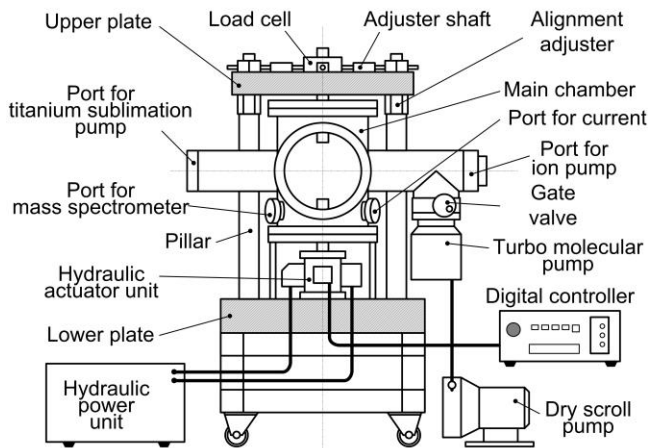
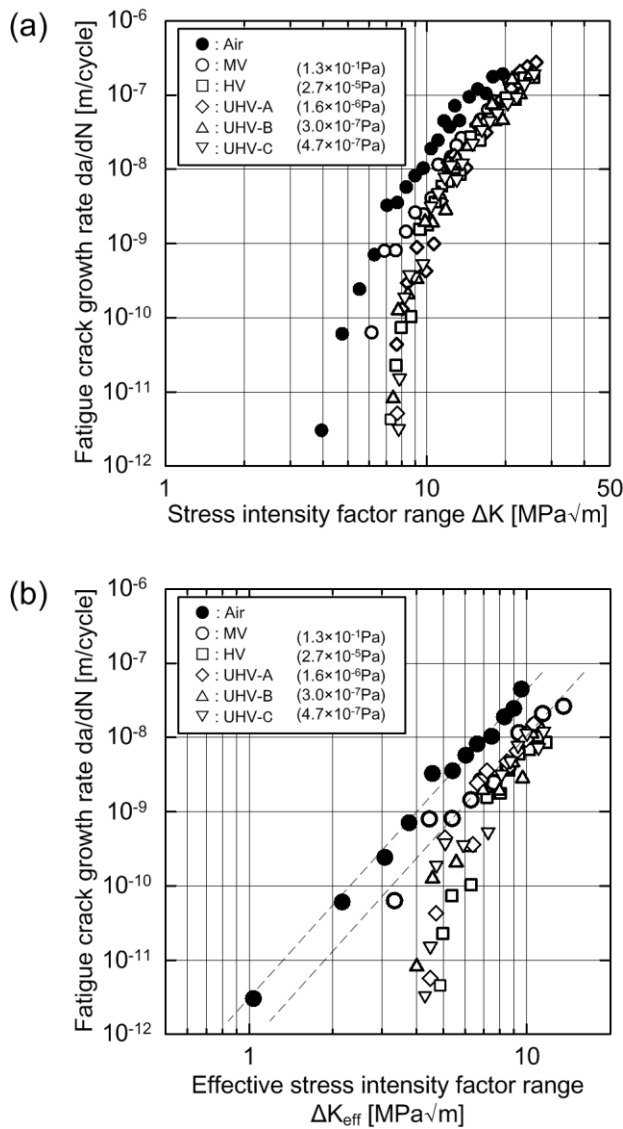


**Fig. 4.** Ultra high vacuum fatigue testing machine.

### 3. Experimental results

Fig. 5a presents the relation between crack propagation rate ( $da/dN$ ) and stress intensity factor range ( $\Delta K$ ) in the different environments. The filled and open symbols indicate the data obtained in air and vacuum, respectively. The crack propagation rates decrease with decreasing the stress intensity factor ranges. The  $da/dN$  in air are greater than those in vacuum at the same  $\Delta K$ . For the small stress intensity factor range,  $\Delta K \leq 10 \text{ MPa}\sqrt{\text{m}}$ , the  $da/dN$  in vacuum decreases dramatically and fatigue cracks in vacuum propagate 1/3 to 1/100 times slower than those in air. Among the test results in vacuum, the crack propagation rates in HV ( $\sim 10^{-5} \text{ Pa}$ ) and UHV ( $\sim 10^{-7} \text{ Pa}$ ) are slower than the rate in MV ( $\sim 10^{-1} \text{ Pa}$ ). The threshold stress intensity factor ranges ( $\Delta K_{th}$ ) are; Air:  $4 \text{ MPa}\sqrt{\text{m}}$ , MV:  $6 \text{ MPa}\sqrt{\text{m}}$ , HV:  $7.2 \text{ MPa}\sqrt{\text{m}}$ , and UHV(A, B and C):  $7.8 \text{ MPa}\sqrt{\text{m}}$ . The  $\Delta K_{th}$  became larger with decreasing vacuum pressure.

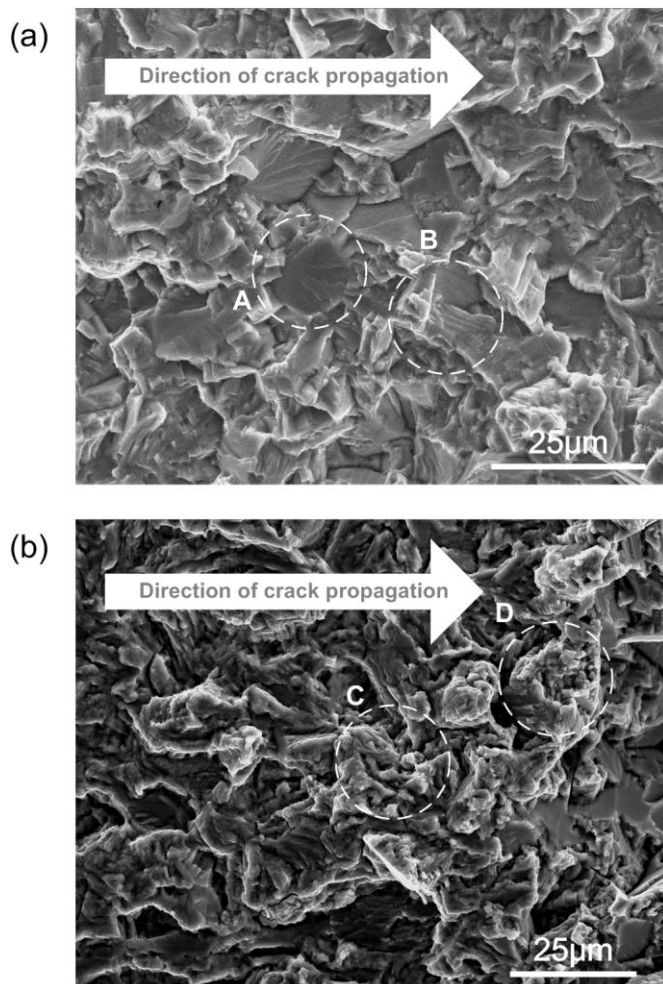
The effective stress intensity factor range ( $\Delta K_{\text{eff}}$ ) was calculated using the crack opening load. Fig. 5b shows the relation between  $da/dN$  and  $\Delta K_{\text{eff}}$ . In air and MV, when  $\Delta K_{\text{eff}}$  became smaller, a commensurate decrease in  $da/dN$  was observed on the double logarithmic chart. On the other hand,  $da/dN$  plunges at  $\Delta K_{\text{eff}} \approx 8 \text{ MPa}\sqrt{\text{m}}$  in HV and UHV, and shows different tendency to that in air and MV. The threshold of  $\Delta K_{\text{eff}}$  in air is about  $1 \text{ MPa}\sqrt{\text{m}}$ , and that in HV and UHV is about  $4 \text{ MPa}\sqrt{\text{m}}$ . This result indicates that the difference of crack propagation rate between in air and in vacuum cannot be explained only by the crack closure.



**Fig. 5.** Results of fatigue crack propagation tests, (a)  $da/dN$ - $\Delta K$  and (b)  $da/dN$ - $\Delta K_{\text{eff}}$ .

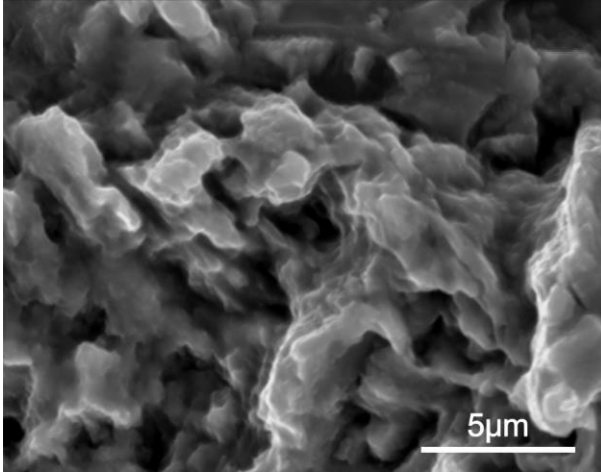
#### 4. Fracture surface observations

Fig. 6 shows a magnified fracture surface where the fatigue crack propagation is strongly affected by microstructure such as grains or grain boundaries around crack tip. In K-decreasing test, the fracture surface is observed near the point where a fatigue crack stopped [10]. Regardless of the test environment, fracture surfaces shows rough features, nevertheless, the detail characteristics are different between the environments. Plane facets, sharp edges of crystallographic jagged pattern and clear slip marks were observed on the fracture surfaces obtained in air and MV as indicated by A and B in Fig. 6a. On the other hand, in HV and UHV, the fracture surfaces show more ductile feature than those in air on the whole. In addition, a distinctive granular feature characterized by a few micrometer size concave-convex was observed as in the dashed circles C and D (Fig. 6b).



**Fig. 6.** Fracture surfaces of the crack propagation tests, (a) Air ( $K = \Delta 7 \text{ MPa}\sqrt{\text{m}}$ ) and (b) HV ( $2.7 \times 10^{-5} \text{ Pa}$ ,  $\Delta K = 8 \text{ MPa}\sqrt{\text{m}}$ ).

An example of the granular region obtained in HV is shown in Fig. 7. From the observation results, it can be concluded that a vacuum pressure affects fatigue crack propagation properties, especially the formation of granular region. The morphological feature in HV and UHV is quite similar to that observed in the sub-surface fractures, as shown in Fig. 1. This indicates that the mechanism of the formation of granular region in the sub-surface fracture is the same as that in the vacuum environments.



**Fig. 7.** Granular region on the fracture surface of crack propagation test (HV,  $2.7 \times 10^{-5}$  Pa,  $\Delta K = 7$  MPa $\sqrt{\text{m}}$ ).

## 5. Discussion

In previous studies, it is reported that the granular region is formed under the condition of vacuum or similar environments and repeated contacts of the fracture surfaces [6-9]. One of the differences between air and vacuum environments is the difference of gas adsorption. Amount of the gas molecules that adsorb on the fracture surface will be estimated based on the adsorption isotherm equation that relates the surface coverage to gas pressure at equilibrium and a fixed temperature. The coverage of molecules was calculated from the following Langmuir equation [11];

$$\theta = \frac{v_a}{v_s} = \frac{P}{P + P_0(T)} \quad (1)$$

$$P_0(T) = k_B T \left( \frac{2\pi m k_B T}{h^2} \right)^{\frac{3}{2}} \exp\left( -\frac{\varepsilon}{k_B T} \right) \quad (2)$$

where  $\theta$ : the fraction coverage of the surface,  $v_a$ : the volume of adsorbate,  $v_s$ : the volume of

adsorbate required to form a monolayer on the adsorbent,  $P$ : pressure [Pa],  $h$ : Planck's constant ( $6.62 \times 10^{-34}$  J·s),  $k_B$ : Boltzmann's constant ( $1.38 \times 10^{-23}$  J/K),  $m$ : the mass of the adsorbed molecule [kg],  $\epsilon$ : the adsorption energy of the adsorbed molecule [J/-].

The calculation was based on the assumption that the all adsorbed gas was oxygen, and the adsorption heat of 988 kJ/mol ( $\text{Ti-O}_2$ ) was used. The relation between the fraction of surface coverage and vacuum pressure is shown in Fig. 8. The surface coverage is almost 100 % between  $10^5$  to  $10^1$  Pa, and decrease rapidly with vacuum pressure. Finally, it approaches asymptotically to 0 % around  $10^6$  Pa.

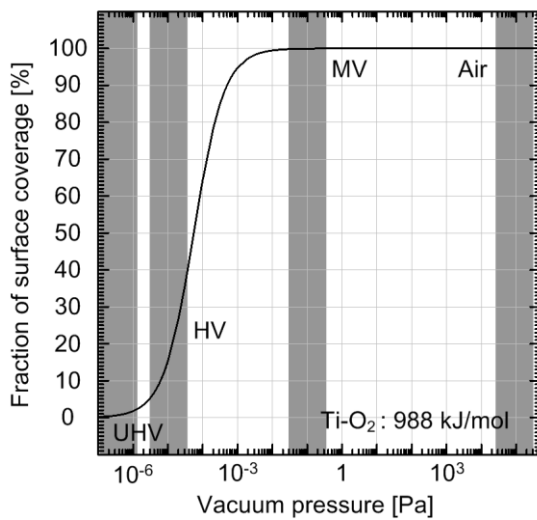


**Fig. 8.** Relation between the fraction of surface coverage and vacuum pressure.

In the fracture surface observations, the granular region existed only on the fracture surfaces obtained in HV and UHV. According to the Fig. 8, it is estimated that the surface coverage were about 100 % for air ( $\sim 10^5$  Pa) and MV ( $\sim 10^1$  Pa), about 20 % for HV ( $\sim 10^3$  Pa), and less than 5 % for UHV ( $10^6$ – $10^7$  Pa), respectively. There is a possibility that newly-formed fracture surfaces, which are partially uncovered with adsorbed gas molecules, appear only in HV and UHV.

On the other hand, the fine concave-convex feature on fracture surfaces has also been confirmed in the sub-surface fractures of high strength steels and aluminum alloys [12, 13]. Additionally, structural refinements of microstructures during the formations of the fine concave-convex feature were pointed out [13, 14]. In this study, the following mechanism of the formation of granular region as shown in Fig. 9 is developed. The direct metal-metal contacts can occur during the unloading process, causing cold-welding (re-bonding) at the contact surfaces [15-17]. During the process, microstructure refinement can also occur near the crack surfaces. In following loading process, the fracture will not necessarily occur at the same

position, and the result can be appearance of a fine asperity on the crack surfaces.

The difference of crack propagation rate between in air and in vacuum, as shown in Fig. 5, could not be fully understood by the crack closure. The cold-welding in vacuum that relates to the formation of the granular region can decrease crack propagation rates, and explain the tendency in HV and UHV that  $da/dN$  plunged at lower  $\Delta K_{eff}$ .

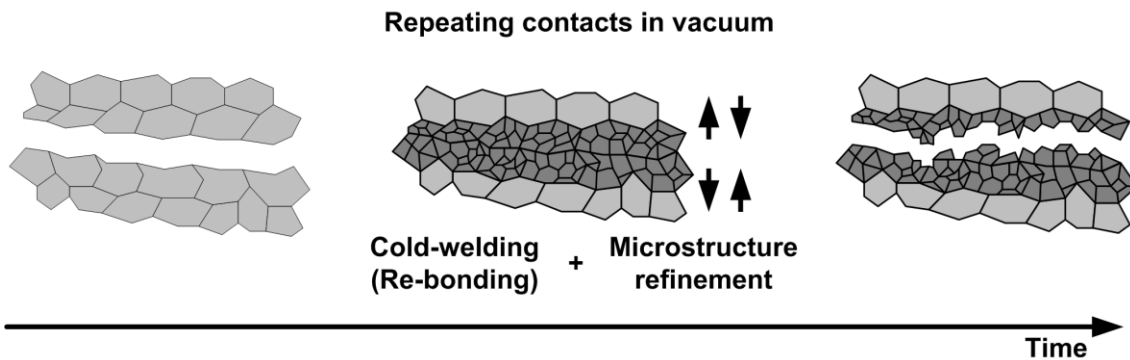


**Fig. 9.** Model of the formation of a granular region based on the cold-welding (re-bonding).

## 6. Summary and conclusions

To determine the effects of vacuum environment on fatigue crack propagations in a Ti-6Al-4V alloy, K-decreasing tests with compact tension (CT) specimens were conducted in air and vacuum environments. A mechanism of formation of the granular region that characterizes crack propagation properties of the sub-surface fracture in very high cycle fatigue was also discussed. Crack propagation rates became slower and threshold stress intensity factor ranges became larger with decreasing vacuum pressure. The tendency cannot be explain only by the crack closure. Observation of fracture surfaces revealed that the granular region which shows a distinctive granular feature characterized by a few micrometer size concave-convex is observed only on the fracture surfaces obtained in high and ultra high vacuum ( $P < 10^{-5}$  Pa). It is suggested that the formation of the granular region correlate strongly with the fraction of surface coverage of adsorbed gas on fracture surfaces. Based on the results, a morphogenetic mechanism with the cold-welding for the formation of the fine asperities of the granular region was introduced. The mechanism can explain the tendency of slower crack propagation in vacuum environments compared to those in ambient air, and the tendency in  $da/dN$ - $\Delta K_{eff}$  relation that could not be explained only by the crack closure.

## References

- [1] G. Schroeder, J. Albrecht, G. Luetjering, Fatigue crack propagation in titanium alloys with lamellar and bi-lamellar microstructures, Material Science and Engineering, A319-321 (2001)

602-604.

- [2] R.K. Nalla, B.L. Boyce, J.P. Campbell, J.O. Peters and R.O. Ritchie, Influence of Microstructure on High-Cycle Fatigue of Ti-6Al-4V: Bimodal vs. Lamellar Structures, *Metall. Mater. Trans. A*, Vol.33A (2002) 899-918.
- [3] Neal, D. F., and Blenkinsop, P. A., Internal fatigue origins in  $\alpha$ - $\beta$  titanium alloys, *Acta Metallurgica*, Vol. 24 (1976) 59-63.
- [4] Oguma, H. and Nakamura, T., The effect of microstructures on interior-originating fatigue fracture of Ti-6Al-4V in gigacycle region, *Proc. of 10<sup>th</sup> World Conference on Titanium (Ti-2003)*, Science and Technology (2003), pp. 1783-1790.
- [5] H. Oguma and T. Nakamura, The effect of microstructure on very high cycle fatigue properties in Ti-6Al-4V, *Scripta Materialia* 63 (2010) 32-34.
- [6] Nakamura, T. and Oguma, H., Effects of vacuum like environment around interior crack on gigacycle fatigue properties, *Proc. of the Materials Science & Technology 2008 Conference, MS&T'08 (2008) CD-ROM*.
- [7] Nakamura, T., Oguma, H., Yamashita, R., A Mechanism of Interior-Originating Fatigue of Ti-6Al-4V Based on Crack Growth Behavior in a High Vacuum, *Proc. of 11<sup>th</sup> World Conference on Titanium (Ti-2007)*, Science and Technology, vol.2 (2007), pp.1225-1228.
- [8] Takashi Nakamura, Hiroyuki Oguma and Yuto Shinohara, The effect of vacuum-like environment inside sub-surface fatigue crack on the formation of ODA fracture surface in high strength steel, *Procedia Engineering*, Vol. 2, Issue 1 (2010) 2121-2129.
- [9] Oguma, H., PhD Thesis, Very High Cycle Fatigue Properties of Ti-6Al-4V Alloy, Hokkaido University (2006).
- [10] B. Oberwinkler, Modeling the fatigue crack growth behavior of Ti-6Al-4V by considering grain size and stress ratio, *Materials Science and Engineering: A*, Vol. 528, Issue 18 (2011) 5983-5992.
- [11] Langmuir, I., The Adsorption of Gases on Plane Surfaces of Glass, Mica and Platinum, *J. Am. Chem. Soc.*, Vol. 40, No. 9 (1918) 1361-1403.
- [12] Y. Murakami, T. Nomoto and T. Ueda, On the mechanism of fatigue failure in the superlong life regime ( $N > 10^7$  cycles). Part I: influence of hydrogen trapped by inclusions, *Fatigue & Fracture of Engineering Materials & Structures*, Vol. 23, Issue 11 (2000) 893-902.
- [13] Akira Ueno, Susumu Miyakawa, Koji Yamada and Tomoyuki Sugiyama, Fatigue behavior of die casting aluminum alloys in air and vacuum, *Procedia Engineering*, Vol. 2, Issue 1 (2010) 1937-1943.
- [14] T. Sakai, Review and Prospects for Current Studies on Very High Cycle Fatigue of Metallic Materials for Machine Structural Use, *J. of Solid Mechanics and Materials Engineering*, Vol. 3 No. 3 Special Issue on M&M2008 (2009) 425-439.

[15] M. Kikukawa, M. Jono and M. Adachi, ASTM STP 675 (1979) 234-253.

[16] R. F. Knarr and R. A. Quon, T. K. Vanderlick, Direct Force Measurements at the Smooth Gold/Mica Interface, Langmuir, Vol. 14 (1998) 6414-6418.

[17] N. A. Alcantar, C. Park, J. Pan, J. N. Israelachvili, Adhesion and coalescence of ductile metal surfaces and nanoparticles, Acta Materialia, Vol. 51 (2003) 31-47.

---

**Fig. 1.** The granular region of the sub-surface fracture (Ti-6Al-4V,  $R = 0.1$ ,  $\sigma_{\max} = 600$  MPa,  $N_f = 5.53 \times 10^7$ ).

**Fig. 2.** Microstructure of Ti-6Al-4V.

**Fig. 3.** Specimen configuration (CT).

**Fig. 4.** Ultra high vacuum fatigue testing machine.

**Fig. 5.** Results of fatigue crack propagation tests, (a)  $da/dN-\Delta K$  and (b)  $da/dN-\Delta K_{\text{eff}}$ .

**Fig. 6.** Fracture surfaces of the crack propagation tests, (a) Air ( $K = \Delta 7$  MPa $\sqrt{m}$ ) and (b) HV ( $2.7 \times 10^{-5}$  Pa,  $\Delta K = 8$  MPa $\sqrt{m}$ ).

**Fig. 7.** Granular region on the fracture surface of crack propagation test (HV,  $2.7 \times 10^{-5}$  Pa,  $\Delta K = 7$  MPa $\sqrt{m}$ ).

**Fig. 8.** Relation between the fraction of surface coverage and vacuum pressure.

**Fig. 9.** Model of the formation of a granular region based on the cold-welding (re-bonding).

**Table 1.** Chemical composition of Ti-6Al-4V (in mass %)

**Table 2.** Mechanical properties of Ti-6Al-4V

**Table 3.** Experimental conditions (Vacuum pressures)